Mode Identification of OAM with Compressive Sensing in the Secondary Frequency Domain

Jin Li and Chao Zhang(✉)

Labs of Avionics, School of Aerospace Engineering,
Tsinghua University, Beijing 100084, People's Republic of China
zhangchao@mail.tsinghua.edu.cn

Abstract. The Electro-Magnetic (EM) waves with Orbital Angular Momentum (OAM) can achieve high spectral efficiency by multiplexing different OAM modes. Different modes are mapped to the frequency shifts in the secondary frequency domain at the receiving end, in order to effectively identify the OAM modes received in partial phase plane. The traditional method requires high-speed acquisition equipment in the process of receiving Radio Frequency (RF) signals directly and its hardware cost is high. Even if analog devices are used for down-conversion to Intermediate Frequency (IF) sampling, the IF bandwidth limits the transmission rate. However, Compressive Sensing (CS) can break the Nyquist restriction by random observation, and is expected to realize the detection and identification of different OAM modes at a lower sampling rate, so that the cost is low. Therefore, this paper proposes an OAM mode identification method based on CS. At the same time, the random sampling is carried out based on the existing hardware device, i.e. Analog-to-Information Converter (AIC), to realize the OAM modes identification with the low sampling rate. The simulation results verify the correctness and effectiveness of the method.

Keywords: Orbital Angular Momentum · Secondary frequency domain · Compressive Sensing · Analog-to-Information Converter · OAM multiplexing · Mode detection and identification

1 Introduction

Orbital Angular Momentum (OAM), as an intrinsic characteristic of electromagnetic wave, is considered as the new dimension of wireless transmission, especially in future mobile communications. Because of the orthogonality between different OAM modes, they can be multiplexed to obtain the higher spectral efficiency

This work is supported by National Natural Science Foundation of China with project number 61731011.

H. Gao et al. (Eds.): ChinaCom 2019, LNICST 312, pp. 301–315, 2020.
https://doi.org/10.1007/978-3-030-41114-5_23

and transmission rate, which makes OAM become an important development direction of Beyond 5th Generation (B5G) and 6th Generation (6G) mobile communications in the future. Besides, OAM can not only increase the capacity by multiplexing, but also improve the transmission performance by Index Modulation (IM) [1]. However, the inverted cone beams and the spiral phase distribution result in the non-zero beam divergent angle. When propagating in free space, the divergence of the non-zero beam angle leads to the increase of the circular energy ring radius in the transverse plane, which makes it difficult for all-phase plane receiving in a long-distance transmission [2]. Therefore, it is necessary to consider partial phase plane reception.

For the partial phase plane receiving method [3], when multiplexing electromagnetic waves with different non-degenerate OAM modes, one-to-one frequency shift can be mapped to the secondary frequency domain by Virtual Rotating Antenna (VRA) [2,4], thus realizing the accurate identification of OAM modes. In Dec. 2016, the 27.5 km electromagnetic wave OAM transmission experiment was successfully completed [5,6]. In Apr. 2018, the same research team also completed a 172 km long ground-to-air transmission experiment from Beijing to Xiong An New Area in the north of Hebei Province, China [7]. However, in the future B5G and 6G high-capacity transmission even with Terahertz, due to the limited sampling rate of our existing hardware devices, it is difficult to meet our transmission rate requirements, or even if high sampling rate can be achieved, the cost is huge. Therefore, how to reduce the sampling rate to identify the OAM mode has become a problem.

The Compressive Sensing (CS) as a new sampling theory [8,9], exploits the sparse characteristics of the signal and uses random sampling to obtain discrete samples of the signal under the condition of the far less than Nyquist sampling rate, and then recovers the signal perfectly through the non-linear reconstruction algorithm [10]. Recently, CS theory has been applied to the detection of Generalized Space Shift Keying (GSSK) symbols in the uncertain Multiple-Input Multiple-Output (MIMO) systems with better performance [11], such as Orthogonal Matching Pursuit (OMP) [12] and the Basis Pursuit (BP) [13]. In addition, in the wake of the related research of the Analog-to-Information Converter (AIC) with Limited Random Sequence (LRS) modulation [14], the required sampling rate may be further reduced.

In this paper, the CS is applied to nondegenerate OAM multiplexing transmissions. Using AIC with LRS modulation as detector through random sampling [14], the low sampling rate with CS can be used to accurately identify OAM modes in the secondary frequency domain, and then high-speed transmission will be achieved. Notably, the method proposed in this paper is able to effectively solve the major problems, i.e., (1) When sampling Radio Frequency (RF) signals directly, the sampling rate is very high, and the hardware equipment is very expensive; (2) Besides, if analog devices are used to down convert the RF signals received by antennas and sample them at Intermediate Frequency (IF), the phase error and attenuation will be caused, which seriously affects our identification of OAM modes. Simultaneously, the sampling rate of the employed data acquisition card limits the data rate of the high-speed transmission.

2 Preliminary Knowledge

In the previous work, it was proposed that the VRA interpolation could be used to detect OAM through the method of the partial phase plane receiving [5]. Processing the signals received by antennas with VRA interpolation will cause the frequency shift in the corresponding transform domain. In this transform domain, different index sets will bring different combinations of OAM modes, different combinations of OAM modes will produce different frequency shifts, but only one spectrum line will be formed. Because it has the same dimension as the traditional frequency domain, we name the transform domain as the secondary frequency domain [4]. Usually, the first frequency domain refers to the traditional frequency domain.

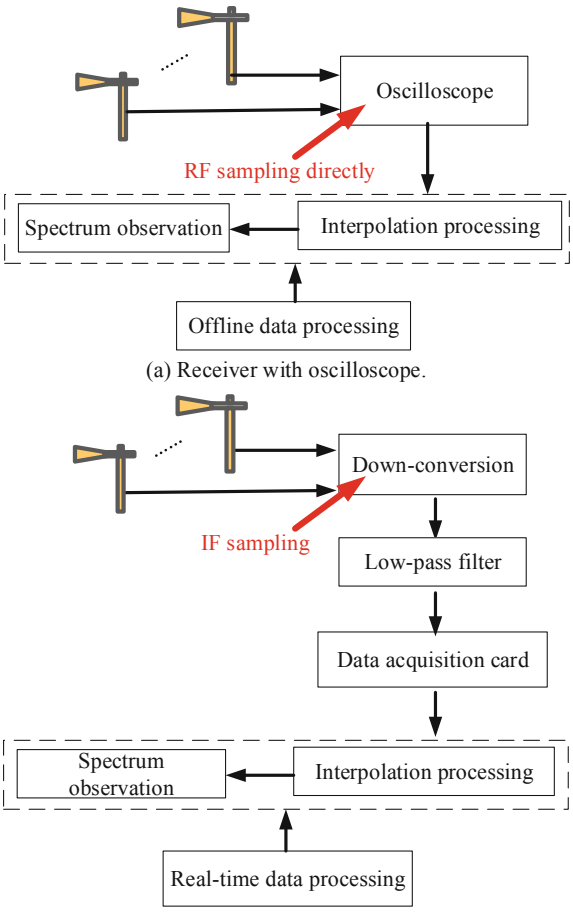

Fig. 1. The comparison of receiver structures based on RF and IF sampling.

In this process, the multiple combinations of different nondegenerate OAM will be converted into the same frequency signal but different frequency shift combinations, which realizes the demodulation and identification of multiplexed OAM modes. Based on VRA, there are two commonly used receiver structures based on RF and IF sampling, as shown in Fig. 1. Specifically, in Fig. 1(a), RF signals are over-sampled directly by the high-speed sampling oscilloscope at the receiving end, and then different OAM modes are converted into the frequency shifts by VRA, which can be used for offline detection of OAM modes. This method has high cost because of the high sampling rate requirements.

In contrast, in Fig. 1(b), the RF signal obtained by the receiver is down-converted to IF with the frequency shifts in the secondary frequency domain. Then, the low-rate data acquisition card is used to identify the real-time OAM modes. However, due to the hardware limitation of the low sampling rate, this method will lead to the lower IF frequency, which will reduce the data carried by IF bandwidth.

3 System Architecture

3.1 System Structure

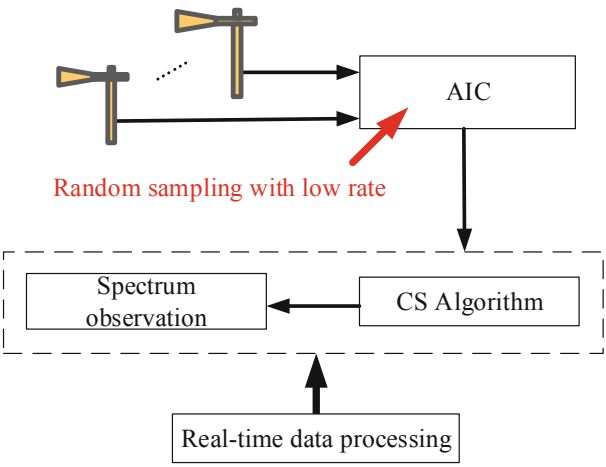

Fig. 2. The receiver structure with AIC.

As we know, CS algorithm can break Nyquist sampling theorem. Because the hardware resources limit RF sampling rate, this paper uses CS algorithm combined with the low sampling rate AIC to effectively replace the high-speed sampling of the oscilloscope, so as to realize the high-speed and accurate identification of OAM modes. Specifically, the RF signals received by antennas are

sampled randomly by AIC, and the spectral line mapped to OAM mode is separated and recovered in the secondary frequency domain by CS, which greatly improves the data transmission rate and avoids the cost of the high-speed sampling device. Figure 2 illustrates the receiver with AIC.

3.2 Analog-to-Information Converter

In this subsection, we review a promising symbol detector for random sampling. AIC with LRS modulation is used at the receiving end, and the structure of AIC with LRS modulation is shown in Fig. 3. It consists of limited random sequence, integrator and low-power Analog-to-Digital Converter (ADC). The AIC differs from the traditional ADC because it can sample the signal randomly. The LRS elements are composed of 1 and 0. The sampler completes the physical process of random sampling well by mixing the sequence of "0" and "1" and integrating the mixed signal. The sequence in length N and consists of M frames, and each frame is in length L. The elements are composed of $N-1$ "0" and only one "1", and the location of 1 is random [14].

The input signal $s(t)$ and the signal $p(t)$ generated by periodic transmission of a finite length random sequence are mixed and the results of mixing are fed into the integrator, where the period of the integrator is the reciprocal of the average sampling rate of the random sampler, and then the integrator is connected to the traditional low-power ADC sampler. The sampling period is also T. In the process of sampling, the random sampling of the analog signal can be realized only by synchronizing the integrator and ADC with the finite length sequence generator. The output $s(n)$ is a discrete signal, which will be sent to the successive real-time data processing module for recovery with CS algorithm.

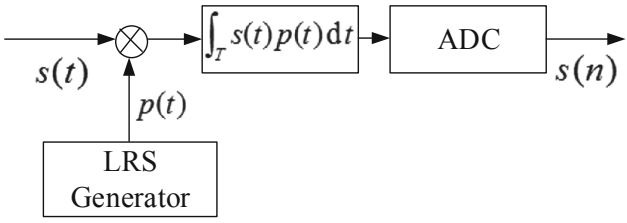

Fig. 3. The structure of AIC with LRS modulation.

3.3 Compressive Sensing Algorithm

The CS technology breaks through the limitation of uniform sampling rate in the traditional Nyquist sampling theorem. For sparse signals, random sampling is used to restore the complete signal with sampling data much less than Nyquist sampling rate [10].

It is precise because AIC random sampling at the receiver can meet the requirement of CS, so that CS algorithm can be used to identify the OAM

modes utilizing the known sparsity. Furthermore, the known sparsity is 1. For CS, greedy algorithms mainly used are Matching Pursuit (MP) algorithm and Orthogonal Matching Pursuit (OMP) algorithm at present.

Specifically, when the measurement matrix is not easy to obtain or unknown, MP algorithm can use greedy iteration algorithm to construct matching dictionary and obtain sparse vectors. Compared with MP algorithm, the improvement of OMP algorithm is that it can accelerate the convergence speed of the algorithm by Schmidt orthogonalization of the columns selected in each iteration. For OAM modes identification, the measurement matrix is known and the real-time demodulation needs to be guaranteed. Thereby, OMP algorithm is considered and employed in this paper [15].

4 Mathematical Model

As mentioned above, assuming that N data symbols are transmitted, then $\mathbf{x}$ can be expressed as the symbol vector of the transmitter

$$\mathbf{x} = [x_0, x_1, ..., x_{N-1}]^{\mathrm{T}}. \tag{1}$$

If the l-th OAM mode needs to be generated, the phase shifting vector $\mathbf{W}$ of the each element in Uniform Circular Array (UCA) composed of N arrays can be denoted as

$$\mathbf{W} = [1, e^{j\frac{2\pi l}{N}}, ..., e^{j\frac{2\pi l(N-1)}{N}}]^{\mathrm{T}}, \tag{2}$$

where $j = \sqrt{-1}$ is the imaginary unit.

Therefore, the received signal $\mathbf{s}$ with M elements at the antenna array can be expressed as

$$\mathbf{s} = \mathbf{HWx} + \mathbf{N}, \tag{3}$$

where $\mathbf{N}$ represents the independent identically distributed Gaussian white noise vector, $\mathbf{H}$ is the channel matrix from the transmitter to the receiver in free space [16,18].

According to Fig. 3, the signal through AIC with LRS modulation denoted as follows

$$\mathbf{s}(n) = \int_T \mathbf{s}(t)\mathbf{p}(t)\mathrm{d}t. \tag{4}$$

It is well known that the recover process of OMP is to reconstruct the P-dimensional original signal $\mathbf{z}(t)$ from the known Q-dimensional measurement signal $\mathbf{s}(n)$ and the measurement matrix $\mathbf{\Phi}$. Assuming that the length of signal $\mathbf{z}(t)$ is P, it is sparse under a projection array $\mathbf{\Psi}$, $\mathbf{\Psi} \in P \times P$, only K elements are greater than the threshold ϵ, where K is far less than P, the measured value can be obtained by observing the signal $\mathbf{z}(t)$ on a basis $\mathbf{\Phi}$, $\mathbf{\Phi} \in Q \times P$, then we can get

$$\mathbf{s} = \mathbf{\Phi z} = \mathbf{\Phi \Psi f} = \mathbf{\Theta f}, \tag{5}$$

where, $\mathbf{\Theta} = \mathbf{\Phi}\mathbf{\Psi}$, $\mathbf{\Theta}$ is the sparse representation of the signal, $\mathbf{z}(t)$ is based on projection and $\mathbf{f}$ is the spectrum in the secondary frequency domain. The dimension Q of the measured value in the above Eq. (5) is less than the dimension P of the signal. There are infinite solutions to the equation. It needs exhaustive time to search the correct result. However, this problem can be solved by the minimum norm problem. Usually, the minimum norm problem can be transformed into the following Eq. (6) [19]:

$$\hat{\mathbf{z}} = \min \|\mathbf{z}\|_0 \qquad \text{s.t. } \mathbf{s} = \mathbf{\Phi}\mathbf{z}, \tag{6}$$

where, $\|\|_0$ denotes the zero norm for the vector, that is, the number of non-zero elements in the vector. When considering noise or error, Eq. (6) can be rewritten as

$$\hat{\mathbf{z}} = \min \|\mathbf{z}\|_0 \qquad \text{s.t. } \|\mathbf{s} - \mathbf{\Phi}\mathbf{z}\|_2 \leq \varepsilon, \tag{7}$$

in which ε is a decimal positive number representing the threshold.

Since LRS sequence can satisfy the random sampling requirement of OMP algorithm, OMP algorithm is considered to recover the spectral line in the secondary frequency domain according to the signal after AIC with LRS. Thus, according to [5], the measurement matrix $\mathbf{\Phi}$ can be defined as

$$\mathbf{\Phi} = \mathbf{w}^{\mathrm{T}} = \mathbf{P}^{\mathrm{T}}\mathbf{R}^{-\mathrm{T}}, \tag{8}$$

where $\mathbf{w}$ is matrix of the weighting coefficient for the received signal after AIC, $(\cdot)^{\mathrm{T}}$ denotes the transpose of matrix, $\mathbf{P}$ is the cross-correlation matrix between the received signal and the interpolated signal, and $\mathbf{R}$ is the autocorrelation matrix of the received signal.

5 Performance Evaluation

According to the description in Sects. 3 and 4, an example is proposed to confirm the correctness of the proposed method. Additionally, in order to further analyze the efficiency, we compare the identification probability, the Bit Error Rate (BER) performance and the capacities in three cases, i.e., the cases of RF sampling directly, IF sampling and OMP with AIC.

5.1 Example

The main simulation parameters are listed in Table 1 and results are all conducted with MATLAB R2016a programming platform. Assuming that the separated OAM Mode 1 and OAM Mode 2 are respectively generated for index keying transmission at the transmitter, and the 100 MHz IF signal is up-converted to 10 GHz RF, fed to the UCA composed of 16 array elements, then received by two antennas placed at the receiving energy ring through the partial phase plane method at the receiver. The receiver will restore spectral lines according to the

index set of the different OAM combinations. Figure 4 illustrates the signals received by Antenna 1 and Antenna 2 for OAM Mode 1, and Fig. 5 shows the signals received by Antenna 1 and Antenna 2 for Mode 2.

Table 1. Simulation parameters.

Parameters	Value
Carrier frequency f	10 GHz
Modulation scheme	QPSK
Signal length	128
Beam divergence angle	2°
Transmission distance	100 m
UCA radius	9 cm
Element number in UCA	16
Receiver ring radius	3.49 m
Receiver antennas space	1 m
OAM modes	1, 2
Sampling rate	1.25 GHz

The limited random sequence $\mathbf{p}(t)$ designed is shown in Fig. 6. The length of the signal is 128, and consists of 16 frames, each frame is in length 8. Then, the measurement signals utilized by CS for OAM Mode 1 after AIC with LRS can be shown in Fig. 7, and the measurement signals used by CS for OAM Mode 2 after AIC with LRS can be shown in Fig. 8. Both low-rate measurement signals will be applied to recover the spectrum line in the secondary frequency domain.

According to the known sparsity of 1 and the measurement signals, the reconstruction is carried out by combining OMP algorithm. Finally, the recovered signal can be converted to a spectral line in the secondary frequency domain, so that separated Mode 1 and Mode 2 are respectively converted to frequency shift in the secondary frequency domain. As shown in Fig. 9, the index of the different OAM mode will be obtained based on the different frequency shift.

As we all know, if the Nyquist sampling is used, two sampling points at least are required for each signal period, so for this example, there are at least 26 sampling points. However, 16 sampling points have been used to realize the low-rate sampling of 10 GHz RF signal and reconstruct the spectrum line in the secondary frequency domain, so that OAM mode identification is achieved. Thus, the method of AIC with CS proposed in this paper has been verified.

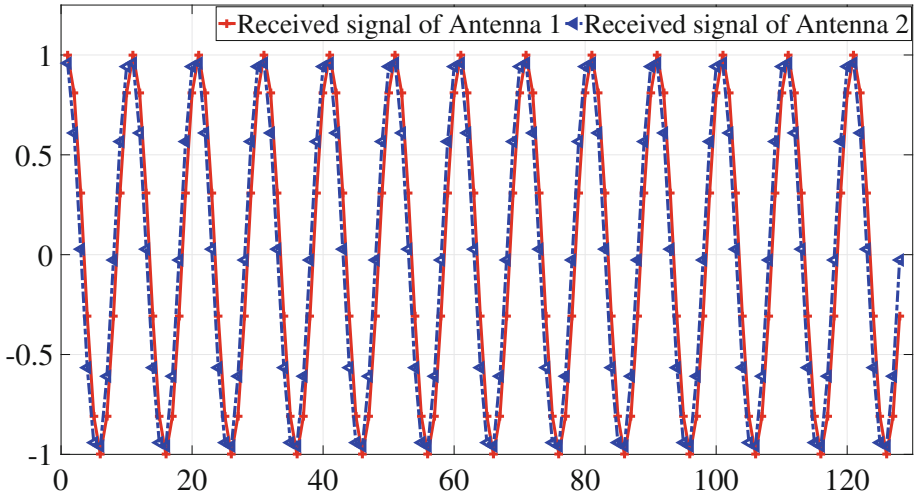

Fig. 4. Typical received signals of Antenna 1 and 2 for Mode 1.

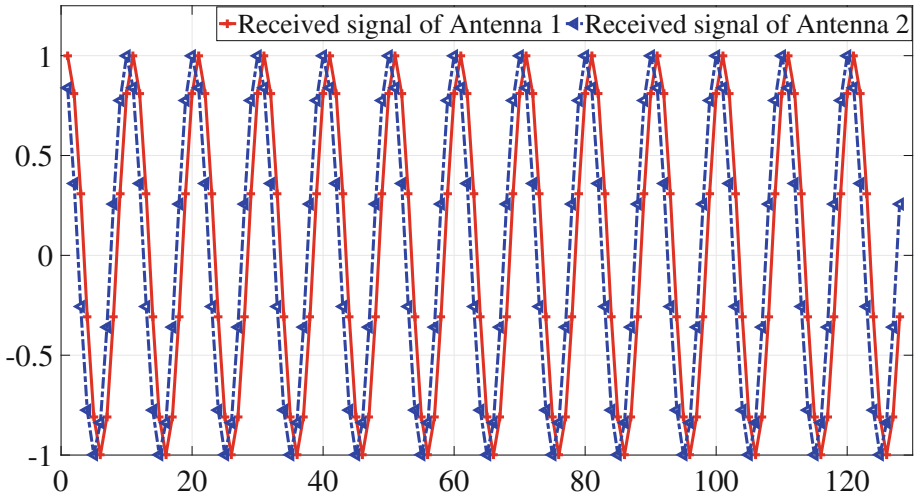

Fig. 5. Typical received signals of Antenna 1 and 2 for Mode 2.

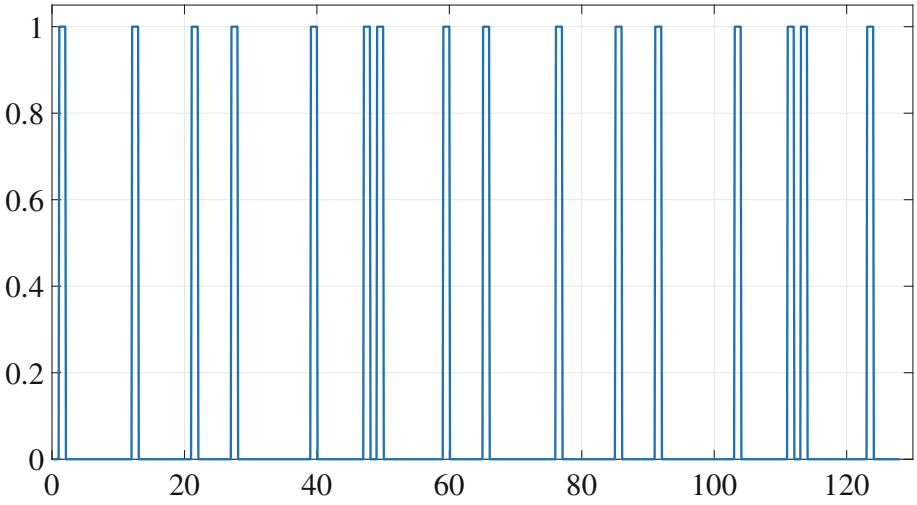

Fig. 6. Typical figure of the limited random sequence $\mathbf{p}(t)$.

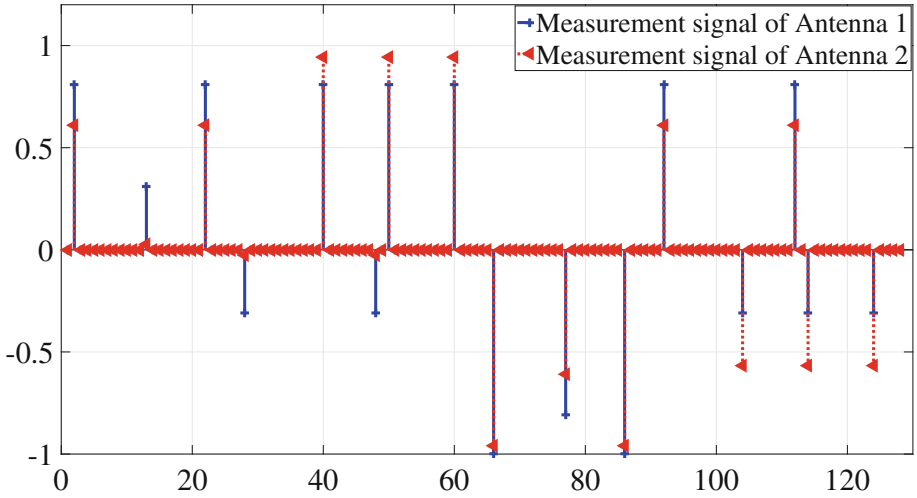

Fig. 7. Typical measurement signals used by CS for Mode 1 after AIC.

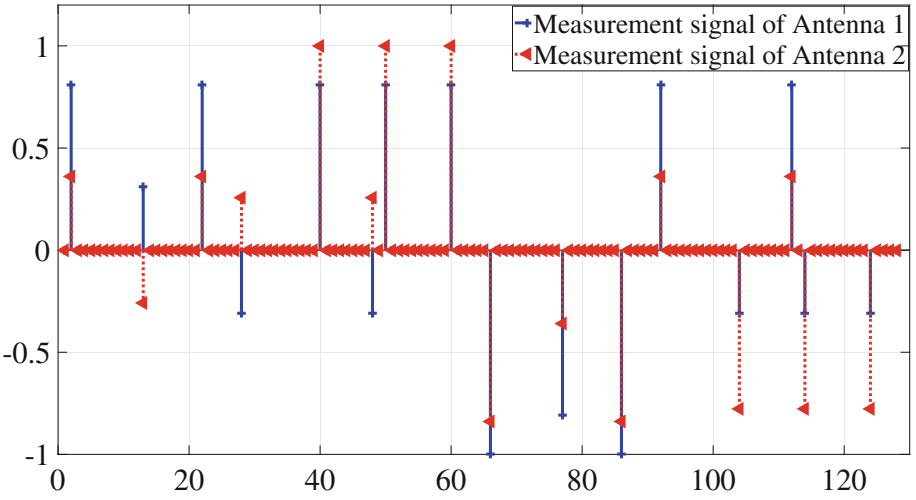

Fig. 8. Typical measurement signals used by CS for Mode 2 after AIC.

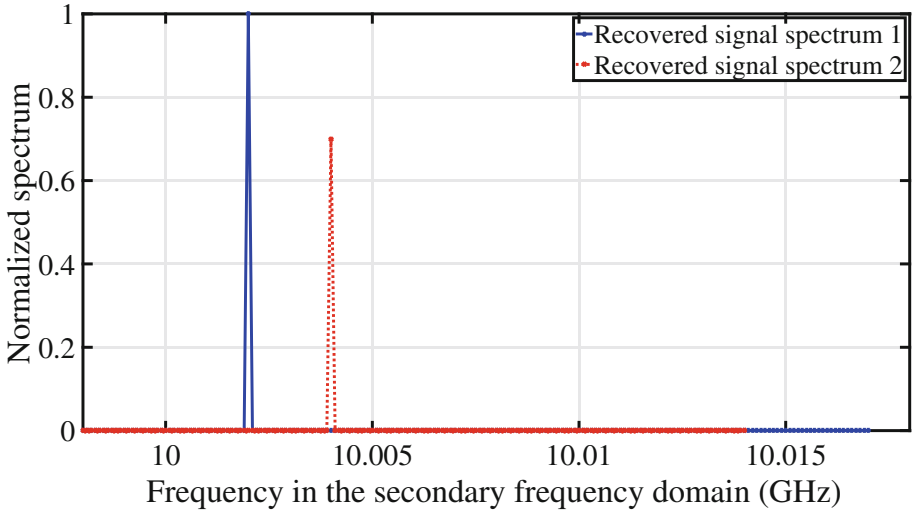

Fig. 9. The spectrum in the secondary frequency domain.

5.2 Analysis

Comparison of Analog Devices. If 10 GHz RF signal is sampled, several points need to be taken in a sampling period in order to recover the signal well, but the cost of such a high sampling oscilloscope is extremely high than the method of IF sampling and OMP with AIC. What's more, if the downconversion is adopted, the sampling rate of the data acquisition card is up to 1.25 GHz, which limits the bandwidth of IF. However, due to the requirement of low sampling rate, higher bandwidth can be obtained through OMP with AIC compared with IF sampling, and then higher data transmission rate can also be achieved.

Simulation Results. Figure 10 demonstrates that when SNR increases, identification probability P_{I} increases quickly. It can be noted that when the SNR reaches about 19 dB, the identification probability of the proposed method in this paper will approach 1, which is superior to the traditional IF sampling. The lower the out-of-band interference ratio is, the higher the identification probability of OAM is. Besides, if the out-of-band interference ratio is as low as 0.001, the identification probability of IF sampling is very close to that of RF sampling and OMP with AIC. Especially, when P_{I} is greater than the threshold probability $P_0 = 0.89$, this method will work well.

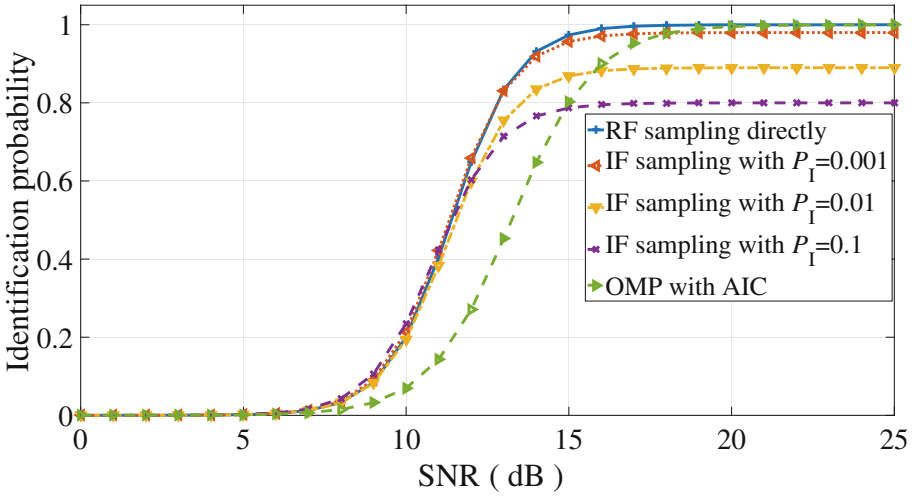

Fig. 10. Identification probability varys with SNR.

According to the identification probability P_{I}, the P_{BER} can be obtained as

$$P_{\mathrm{BER}} = 1 - P_{\mathrm{I}}. \tag{9}$$

Therefore, the BER performance simulation is shown in Fig. 11, the highest BER performance of IF sampling can be found under certain SNR, and the BER performance of OMP with AIC is fairly better than IF sampling.

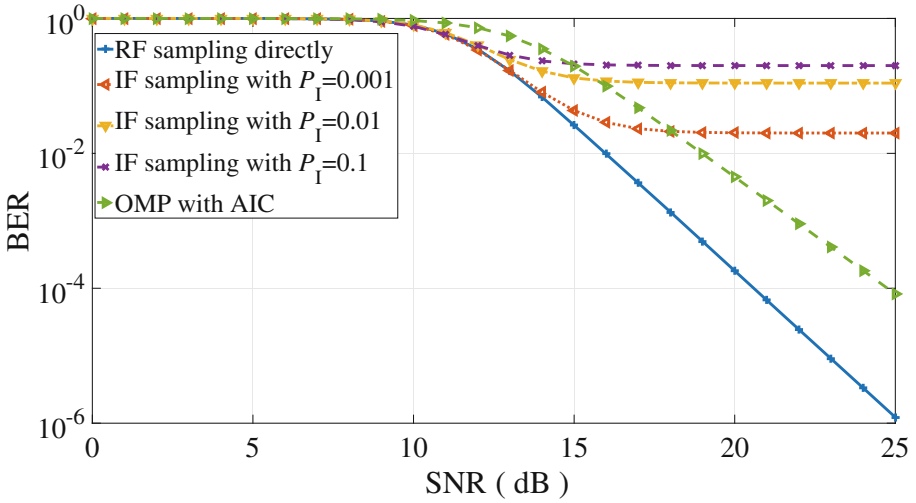

Fig. 11. The BER performance simulation results vary with SNR.

For a communication system, the transmission capacity is also a extremely important evaluation index. Consequently, Fig. 12 illustrates the capacity curve as BER changes according to the Shannon formula and BER curve, the capacity curve of OMP with AIC is close to the RF sampling directly.

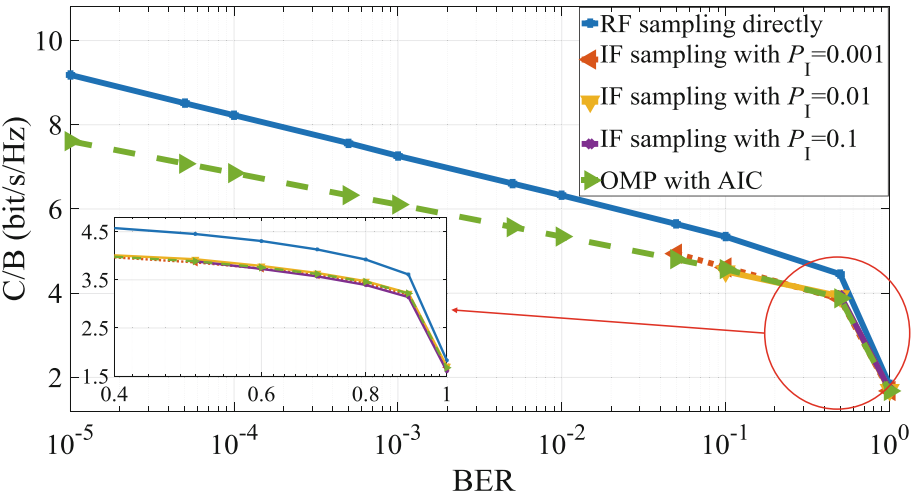

Fig. 12. The transmission capacity simulation comparison.

Overall, OMP with AIC is able to be used for random sampling at a fairly low sampling rate, which is of great benefit to replace the high-speed sampling scheme. However, the sampling equipment with AIC increases the difficulty. Then, the trade-off should be considered in the practical application.

6 Conclusion

The proposed method in this paper, which combines CS algorithm with low sampling rate AIC, has been effectively applied to the accurate identification of OAM modes. Furthermore, the correctness and efficiency of this method are confirmed through an example and some analysis, such as comparison of analog devices, identification probability, BER and capacity. Moreover, with the coming of next generation mobile communications (B5G and 6G), the wireless high-speed transmission even to 1 Tbps with low sampling rate becomes a promising topic. Evidently, the proposed method is significant to promote the transmission capacity with low sampling rate AIC hardware equipment in the future.

References

1. Basar, E.: Orbital angular momentum with index modulation. IEEE Trans. Wirel. Commun. **17**(3), 2029–2037 (2018)
2. Zhang, C., Ma, L.: Millimetre wave with rotational orbital angular momentum. Sci. Rep. **6**, 31921 (2016)
3. Zhang, W., Zheng, S., Chen, Y., et al.: Orbital angular momentum-based communications with partial arc sampling receiving. IEEE Commun. Lett. **20**(7), 1–1 (2016)
4. Zhao, Y., Jiang, J., Jiang, X., et al.: Orbital angular momentum multiplexing with non-degenerate modes in secondary frequency domain. In: IEEE MTT-S International Wireless Symposium (IWS), Chengdu, pp. 1–4 (2018)
5. Zhang, C., Ma, L.: Detecting the orbital angular momentum of electro-magnetic waves using virtual rotational antenna. Sci. Rep. **7**(1), 4585 (2017)
6. Zhang, C., Chen, D., Jiang, X.: RCS diversity of electromagnetic wave carrying orbital angular momentum. Sci. Rep. **7**(1), 15412 (2017)
7. Zhang, C., Zhao, Y.: Orbital angular momentum nondegenerate index mapping for long distance transmission. IEEE Trans. Wirel. Commun. **29**(2), 7672 (2019)
8. Donoho, D.L.: Compressed sensing. IEEE Trans. Inf. Theory **52**(4), 1289–1306 (2006)
9. Ding, W., Yang, F., Dai, W., et al.: Time-frequency joint sparse channel estimation for MIMO-OFDM systems. IEEE Commun. Lett. **19**(1), 58–61 (2014)
10. Jiang, J., Chen, C.: Analysis in theory and technology application of compressive sensing. In: 2014 Sixth International Conference on Intelligent Human-Machine Systems and Cybernetics, Hangzhou, pp. 184–187 (2014)
11. He, L., Wang, J., Ding, W., Song, J.: ℓ_∞Minimization based symbol detection for generalized space shift keying. IEEE Commun. Lett. **19**(7), 1109–1112 (2015)
12. Yu, C.M., Hsieh, S.H., Liang, H.W., et al.: Compressed sensing detector design for space shift keying in MIMO systems. IEEE Commun. Lett. **16**(10), 1556–1559 (2012)

13. Liu, W., Wang, N., Jin, M., Xu, H.: Denoising detection for the generalized spatial modulation system using sparse property. IEEE Commun. Lett. **18**(1), 22–25 (2014)
14. Zhang, C., Wu, Z., Xiao, J.: Adaptive analog-to-information converter with limited random sequence modulation. In: 2011 International Conference on Wireless Communications and Signal Processing (WCSP), Nanjing, pp. 1–5 (2011)
15. Tropp, J.A., Gilbert, A.C.: Signal recovery from random measurements via orthogonal matching pursuit. IEEE Trans. Inf. Theory **53**(12), 4655–4666 (2007)
16. Jackson, J.D.: Classical Electrodynamics. Wiley, New York (1999)
17. Zhang, W., Zheng, S., Hui, X., et al.: Mode division multiplexing communication using microwave orbital angular momentum: an experimental study. IEEE Trans. Wirel. Commun. **16**(2), 1308–1318 (2017)
18. Jiang, X., Zhao, Y., Jiang, X., Zhang, C.: Capacity evaluation on the long-distance orbital angular momentum non-orthogonal transmission. In: IEEE MTT-S International Wireless Symposium (IWS), Chengdu, pp. 1–4 (2018)
19. Li, H., Zhang, Q., Cui, A., et al.: Minimization of fraction function penalty in compressed sensing. IEEE Trans. Neural Netw. Learn. Syst. 1–12 (2017)